AD-A134 490 ANALYSIS OF FIN-LINES WITH THE FINITE METALLIZATION TTHICKNESS(U) ILLINOIS UNIV AT URBANA ELECTROMAGNETICS LAB T KITAZAWA ET AL. OCT 83 UIEM-83-11 ARO-18054.8-EL 1/1

UNCLASSIFIED DAAG29-82-K-0084 F/G 9/5 NL

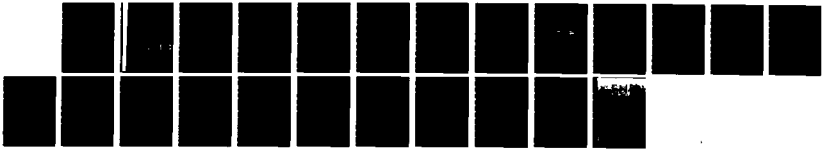

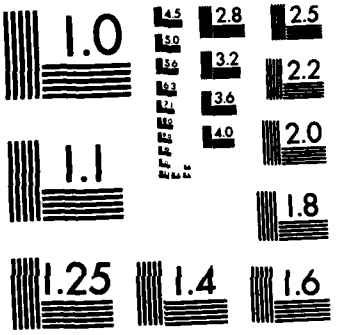

ANALYSIS OF FIN-LINES WITH THE FINITE METALLIZATION THICKNESS

INTERIM TECHNICAL REPORT

T. Kitazawa
R. Mittra

October 1983

SUPPORTED IN PART BY

U. S. ARMY RESEARCH OFFICE

GRANT NO. DAAG29-82-K-0084

ELECTROMAGNETICS LABORATORY
DEPARTMENT OF ELECTRICAL ENGINEERING
ENGINEERING EXPERIMENT STATION
UNIVERSITY OF ILLINOIS AT URBANA-CHAMPAIGN
URBANA, ILLINOIS 61801

THE FINDINGS IN THIS REPORT ARE NOT TO BE CONSTRUED AS AN OFFICIAL DEPARTMENT OF THE ARMY POSITION, UNLESS SO DESIGNATED BY OTHER AUTHORIZED DOCUMENTS.

UNCLASSIFIED

SECURITY CLASSIFICATION OF THIS PAGE (When Data Entered)

REPORT DOCUMENTATION PAGE		READ INSTRUCTIONS BEFORE COMPLETING FORM
1. REPORT NUMBER	2. GOVT ACCESSION NO. AD-A134490	3. RECIPIENT'S CATALOG NUMBER
4. TITLE (and Subtitle) ANALYSIS OF FIN-LINES WITH THE FINITE METALLIZATION THICKNESS		5. TYPE OF REPORT & PERIOD COVERED Interim Technical Report
		6. PERFORMING ORG. REPORT NUMBER EM 83-11; UILU-ENG-83-2556
7. AUTHOR(s) T. Kitazawa R. Mittra		8. CONTRACT OR GRANT NUMBER(s) Supported in part by DAAG29-82-K-0084
9. PERFORMING ORGANIZATION NAME AND ADDRESS Electromagnetics Laboratory Department of Electrical Engineering University of Illinois, Urbana, Illinois 61801		10. PROGRAM ELEMENT, PROJECT, TASK AREA & WORK UNIT NUMBERS P18054-EL
11. CONTROLLING OFFICE NAME AND ADDRESS U. S. Army Research Office P. O. Box 12211 Research Triangle Park, N.C. 27709		12. REPORT DATE October 1983
		13. NUMBER OF PAGES 20
14. MONITORING AGENCY NAME & ADDRESS(if different from Controlling Office)		15. SECURITY CLASS. (of this report) UNCLASSIFIED
		15a. DECLASSIFICATION/DOWNGRADING SCHEDULE

16. DISTRIBUTION STATEMENT (of this Report)

Distribution Unlimited.

Approved for public release.

17. DISTRIBUTION STATEMENT (of the abstract entered in Block 20, if different from Report)

18. SUPPLEMENTARY NOTES

The findings in this report are not to be construed as an official Department of the Army position, unless so designated by other authorized documents.

19. KEY WORDS (Continue on reverse side if necessary and identify by block number)

fin-line; finite metallization thickness; millimeter waveguides; propagation characteristics

20. ABSTRACT (Continue on reverse side if necessary and identify by block number)

In this paper, we present a method for analyzing fin-line structures with finite metallization thicknesses. The method, although it is based on a hybrid mode formulation, by-passes the lengthy process of formulating the determinantal equation for the unknown propagation constant. Some numerical results are presented to show the effect of the metallization thickness for unilateral and bilateral fin lines.

DD FORM 1 JAN 73 1473 EDITION OF 1 NOV 65 IS OBSOLETE

UNCLASSIFIED

SECURITY CLASSIFICATION OF THIS PAGE (When Data Entered)

UILU-ENG-83-2556

Electromagnetics Laboratory Report No. 83-11

ANALYSIS OF FIN-LINES WITH THE FINITE METALLIZATION THICKNESS

by

T. Kitazawa
R. Mittra

Electromagnetics Laboratory
Department of Electrical Engineering
University of Illinois at Urbana-Champaign
Urbana, Illinois 61801

Interim Technical Report

October 1983

Supported in part by

U. S. Army Research Office
Contract No. DAAG29-82-K-0084

TABLE OF CONTENTS

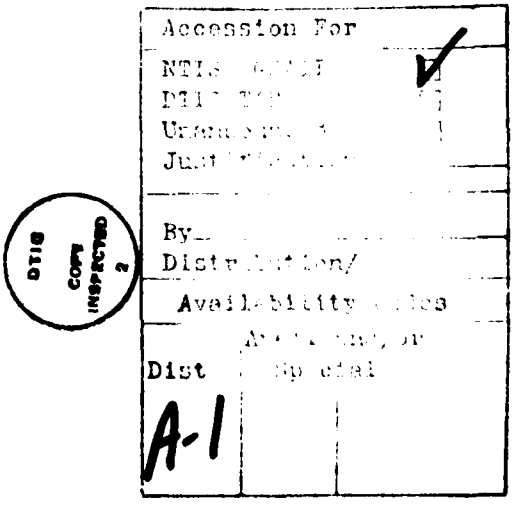

I. INTRODUCTION

Fin-line structures have received considerable attention because of their usefulness as millimeter-wave integrated circuit components. Recently, two efficient numerical methods for analyzing the propagation characteristics of fin-line structures were presented. The first of these employs the spectral domain technique [1], [2], whereas the second utilizes network analytical methods for electromagnetic fields [3]. Both of these methods are based on the hybrid mode formulation as opposed to the TE approximation [4], but they neglect the effect of the metallization thickness, which increases with higher operating frequencies and narrower gaps in the metallization. Hybrid analysis and the effect of the metallization thickness were given for the microwave planar transmission lines [5], [6]; however, the procedure for deriving the Green's functions is rather involved and lengthy. This paper presents an efficient method which circumvents the laborious formulation process for fin-line structures with a finite metallization thickness. Although the method is an extension of the treatment in [3], [5] and [6], it derives Green's functions using the conventional circuit theory rather than by directly solving the differential equations with boundary conditions. Some numerical results are presented and compared with available data.

II. THE NETWORK FORMULATION OF THE PROBLEM

The unilateral fin line shown in Fig. 1 is used to illustrate the formulation procedure, but the method itself is quite general. Application to other structures will be discussed later in this section.

As a first step, we express the transverse (to z) fields in each region by the following spectral representation:

$$\left.\begin{matrix}\bar{E}_t^{(i)}(x,y,z)\\ \bar{H}_t^{(i)}(x,y,z)\end{matrix}\right\} = \sum_{\ell=1}^{2}\sum_{n=0}^{\infty}\left\{\begin{matrix}V_{\ell n}^{(i)}(z)\ \bar{f}_{\ell n}^{(i)}(x)\\ I_{\ell n}^{(i)}(z)\ \bar{g}_{\ell n}^{(i)}(x)\end{matrix}\right\} e^{-j\beta_0 y} \qquad (1)$$

$$i = 1,2,3,4$$

where the vector mode functions $\bar{f}_{\ell n}^{(i)}$ and $\bar{g}_{\ell n}^{(i)}$ in each region are given as:

A) region (1), (3) and (4)

$$\bar{f}_{1n}^{(i)} = \frac{-1}{K_A}\sqrt{\frac{\eta_n}{2A}}\ \{\bar{x}_0\alpha_A \cos(\alpha_A x) - \bar{y}_0 j\beta_0 \sin(\alpha_A x)\}$$

$$\bar{f}_{2n}^{(i)} = \frac{1}{K_A}\sqrt{\frac{\eta_n}{2A}}\ \{\bar{x}_0 j\beta_0 \cos(\alpha_A x) - \bar{y}_0\alpha_A \sin(\alpha_A x)\}$$

$$\bar{g}_{\ell n}^{(i)} = \bar{z}_0 \times \bar{f}_{\ell n}^{(i)} \quad (\ell = 1,2) \qquad (2)$$

$$\alpha_A = \frac{n\pi}{A}\ ,\ K_A = \sqrt{\alpha_A^2 + \beta_0^2}$$

$$\eta_n = \begin{cases}1 & (n=0)\\ 2 & (n\neq 0)\end{cases}$$

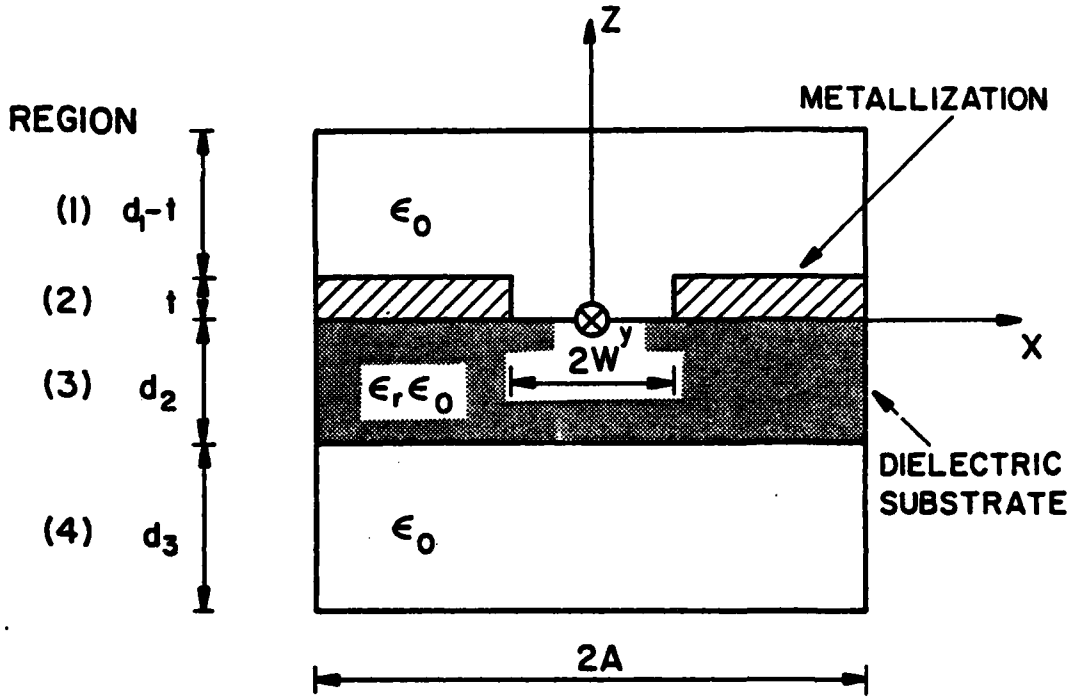

Figure 1. Unilateral fin line.

B) region (2)

$$\bar{f}_{1n}^{(2)} = \frac{-1}{K_W}\sqrt{\frac{\eta_n}{2W}}\ \{\bar{x}_0\alpha_W\cos(\alpha_W x) - \bar{y}_0 j\beta_0\sin(\alpha_W x)\}$$

$$\bar{f}_{2n}^{(2)} = \frac{1}{K_W}\sqrt{\frac{\eta_n}{2W}}\ \{\bar{x}_0 j\beta_0\cos(\alpha_W x) - \bar{y}_0\alpha_W\sin(\alpha_W x)\} \qquad (3)$$

$$\bar{g}_{\ell n}^{(2)} = \bar{z}_0 \times \bar{f}_{\ell n}^{(2)} \quad (\ell = 1,2), \quad \alpha_W = \frac{n\pi}{W}, \quad K_W = \sqrt{\alpha_W^2 + \beta_0^2}$$

where β_0 is the propagation constant, and $\bar{x}_0$, $\bar{y}_0$, and $\bar{z}_0$ are the x-, y-, and z-directed unit vectors, respectively. It should be noted that the vector mode functions $\bar{f}_{\ell n}^{(i)}$, $\bar{g}_{\ell n}^{(i)}$ satisfy the boundary conditions at $x = \pm W$ and $\pm A$ with the following orthonormal properties:

$$\int \bar{g}_{\ell' n'}^{(i)*}(x) \cdot \bar{z}_0 \times \bar{f}_{\ell n}^{(i)}(x)\, dx = \delta_{\ell\ell'}\,\delta_{nn'} \quad (i = 1,2,3,4) \qquad (4)$$

Substituting expression (1) into Maxwell's field equations, we obtain the differential equations for the modal voltages and currents:

$$-\frac{d}{dz} V_{\ell n}^{(i)} = j\kappa^{(i)} z_\ell^{(i)} I_{\ell n}^{(i)}$$

$$-\frac{d}{dz} I_{\ell n}^{(i)} = j\kappa^{(i)} y_\ell^{(i)} V_{\ell n}^{(i)} \qquad (5)$$

where

$$\kappa^{(i)} = \sqrt{\omega^2 \varepsilon^{(i)} \mu_0 - K^{(i)2}}$$

$$\varepsilon^{(i)} = \begin{cases} \varepsilon_r\varepsilon_0 & \text{(region (3))} \\ \varepsilon_0 & \text{(otherwise)} \end{cases} \qquad K^{(i)} = \begin{cases} K_W & \text{(region (2))} \\ K_A & \text{(otherwise)} \end{cases}$$

$$z_1^{(i)} = \frac{\kappa^{(i)}}{\omega\varepsilon^{(i)}} , \qquad z_2^{(i)} = \frac{\omega\mu_0}{\kappa^{(i)}} \tag{6}$$

$$y_\ell^{(i)} = \frac{1}{z_\ell^{(i)}} \qquad (\ell = 1,2)$$

The boundary conditions to be satisfied are expressed as follows:

$$V_{\ell n}^{(1)}(d_1) = 0 \tag{7}$$

$$V_{\ell n}^{(1)}(t+0) = v_\ell^{a+} \tag{8}$$

$$V_{\ell n}^{(2)}(t-0) = v_\ell^{a-} \tag{9}$$

$$V_{\ell n}^{(2)}(+0) = v_\ell^{b+} \tag{10}$$

$$V_{\ell n}^{(3)}(-0) = v_\ell^{b-} \tag{11}$$

$$V_{\ell n}^{(3)}(-d_2+0) = V_{\ell n}^{(4)}(-d_2-0) \tag{12a}$$

$$I_{\ell n}^{(3)}(-d_2+0) = I_{\ell n}^{(4)}(-d_2-0) \tag{12b}$$

$$V_{\ell n}^{(4)}(-d_2-d_3) = 0 \tag{13}$$

and

$$\bar{H}_t^{(1)}(t+0) = \bar{H}_t^{(2)}(t-0) \qquad (|x| \leq W) \tag{14}$$

$$\bar{H}_t^{(2)}(+0) = \bar{H}_t^{(3)}(-0) \qquad (|x| \leq W) \tag{15}$$

where voltage sources v_ℓ^{a+} , v_ℓ^{b+} are given as:

$$\left.\begin{matrix} v_\ell^{a+} \\ v_\ell^{a-} \end{matrix}\right\} = \int_{-W}^{W} \left\{\begin{matrix} \bar{f}_{\ell n}^{(1)*}(x') \\ \bar{f}_{\ell n}^{(2)*}(x') \end{matrix}\right\} \cdot \bar{e}_a(x')\ dx' \tag{16a}$$

$$\left.\begin{matrix} v_\ell^{b+} \\ v_\ell^{b-} \end{matrix}\right\} = \int_{-W}^{W} \left\{\begin{matrix} \bar{f}_{\ell n}^{(2)*}(x') \\ \bar{f}_{\ell n}^{(3)*}(x') \end{matrix}\right\} \cdot \bar{e}_b(x')\ dx' \tag{16b}$$

and where $\bar{e}_a$ and $\bar{e}_b$ are the transverse electric fields at z = t and z = 0, respectively,

$$\begin{matrix} \bar{e}_a \\ b \end{matrix} = \bar{x}_0 \begin{matrix} e_{ax} \\ b \end{matrix} + \bar{y}_0 \begin{matrix} e_{ay} \\ b \end{matrix} \tag{17}$$

Equivalent circuits in the z-direction can be derived by considering the differential equations (5) together with the boundary conditions (7)-(13) (Figure 2). The modal voltages $V_{\ell n}^{(i)}$ and currents $I_{\ell n}^{(i)}$ in each region can be obtained by using conventional circuit theory. Electromagnetic fields in each region can then be derived by substituting $V_{\ell n}^{(i)}$ and $I_{\ell n}^{(i)}$ into (1). Finally, the application of the remaining boundary conditions (14) and (15) results in the following set of equations for the unknown electric fields $\bar{e}_a$ and $\bar{e}_b$ at z = t and z = 0, and for the unknown propagation constant β_0:

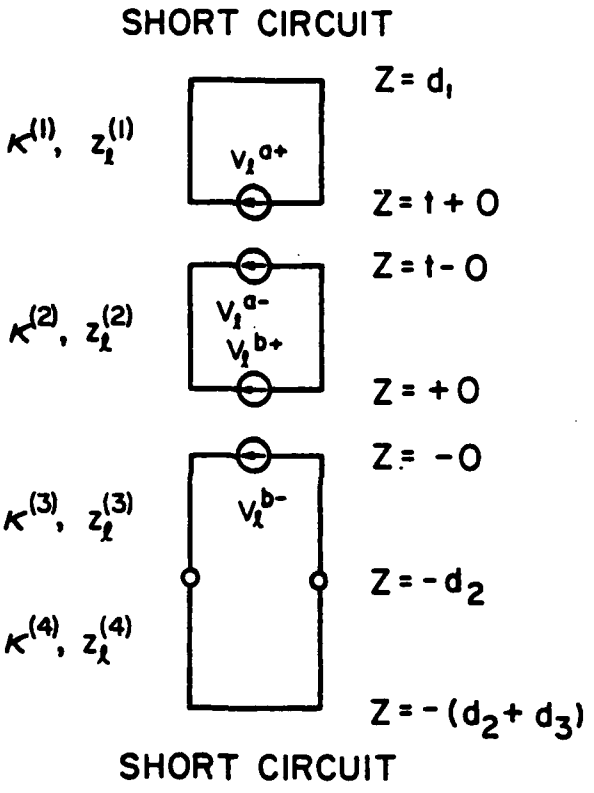

Figure 2. Equivalent circuits for transverse section of fin line.

$$\sum_{\ell=1}^{2}\sum_{n=0}^{\infty}\int_{-W}^{W} Y_\ell^{(1)}(t+0|t)\,\bar{g}_{\ell n}^{(1)}(x)\,\bar{f}_{\ell n}^{(1)*}(x')\cdot\bar{e}_a(x')\,dx'$$

$$= \sum_{\ell=1}^{2}\sum_{n=0}^{\infty}\int_{-W}^{W}\{Y_\ell^{(2)}(t-0|t)\,\bar{g}_{\ell n}^{(2)}(x)\,\bar{f}_{\ell n}^{(2)*}(x')\cdot\bar{e}_a(x') \qquad (18a)$$

$$+ Y_\ell^{(2)}(t-0|0)\,\bar{g}_{\ell n}^{(2)}(x)\,\bar{f}_{\ell n}^{(2)*}(x')\cdot\bar{e}_b(x')\}\,dx'$$

$$\sum_{\ell=1}^{2}\sum_{n=0}^{\infty}\int_{-W}^{W}\{Y_\ell^{(2)}(+0|t)\,\bar{g}_{\ell n}^{(2)}(x)\,\bar{f}_{\ell n}^{(2)*}(x')\cdot\bar{e}_a(x')$$

$$+ Y_\ell^{(2)}(+0|0)\,\bar{g}_{\ell n}^{(2)}(x)\,\bar{f}_{\ell n}^{(2)*}(x')\cdot\bar{e}_b(x')\}\,dx' \qquad (18b)$$

$$= \sum_{\ell=1}^{2}\sum_{n=0}^{\infty}\int_{-W}^{W} Y_\ell^{(3)}(-0|0)\,\bar{g}_{\ell n}^{(3)}(x)\,\bar{f}_{\ell n}^{(3)*}(x')\cdot\bar{e}_b(x')\,dx'$$

where $Y_\ell^{(i)}(z|z')$ are the Green's functions which relate the modal currents $I_\ell^{(i)}(z)$ to the voltage source in each of the three regions. The set of equations (18) is rigorous. Numerical solution of the equations is discussed in the next section.

Before concluding this section, we explain why the present formulation is efficient and why it is convenient to analyze various types of fin-line structures using the present approach. The equivalent circuit for a unilateral fin-line was derived during the formulation process of (18). However, these circuits could have been obtained directly by inspection, without going through the intermediate steps represented by Equations (1) - (13) regardless of the number of gaps and/or dielectric layers in the fin-line. For example, Fig. 3b shows the equivalent circuits for the bilateral fin-line whose geometry is given in Fig. 3a. Once the equivalent circuits are obtained, we can derive the set of equations in (18) by using the

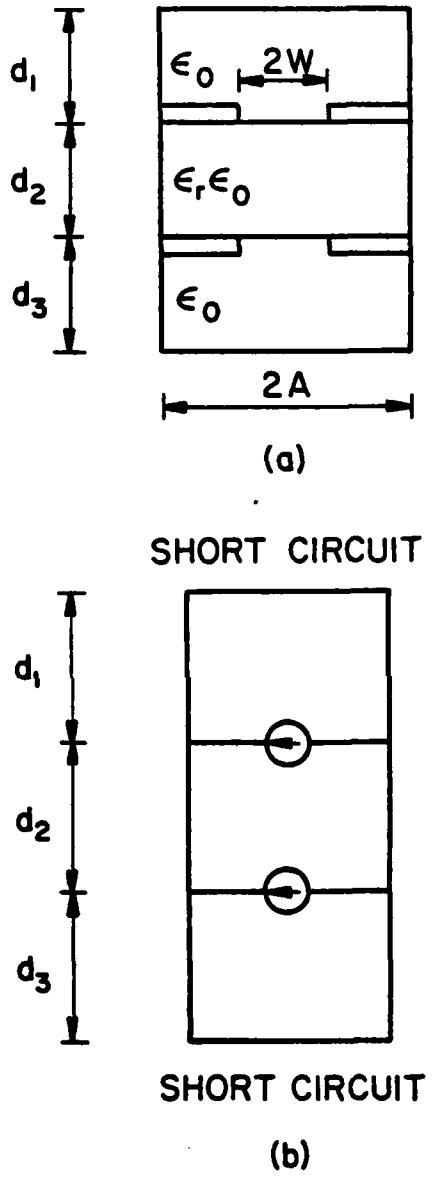

Figure 3. Bilateral fin line (Metalization thickness is neglected in this figure).

conventional circuit theory approach rather than by solving a set of differential equations, together with appropriate boundary conditions.

III. NUMERICAL COMPUTATIONS

The numerical procedure for solving (18) is analogous to that used in [3], [5], [6]; therefore, only a summary of the steps will be given below.

The first step is to expand the unknown electric fields $\bar{e}_a$ and $\bar{e}_b$ at $z = t$ and 0, in terms of an appropriate set of basis functions, e.g.,

$$\left.\begin{matrix} e_{xa}(x) \\ e_{xb}(x) \end{matrix}\right\} = \sum_{k=1}^{2N_x} \begin{Bmatrix} a_{xk} \\ b_{xk} \end{Bmatrix} f_{xk}(x)$$

$$\left.\begin{matrix} e_{ya}(x) \\ e_{yb}(x) \end{matrix}\right\} = j \sum_{k=1}^{2N_y} \begin{Bmatrix} a_{yk} \\ b_{yk} \end{Bmatrix} f_{yk}(x) \qquad (19)$$

where $a_{\substack{xk \\ y}}$ and $b_{\substack{xk \\ y}}$ are the unknown coefficients. The second step is to apply the Galerkin's procedure to Eq. (18), which results in the determinantal equation for the propagation constant β_0. Finally, the determinantal equation is solved for the propagation constant β_0 in the fin line structure. Accurate solutions can be obtained with only a small number of basis functions, if these functions incorporate the edge effect. The following basis functions were used for the numerical results presented in this paper:

$$f_{xk}(x) = \frac{T_{k-1}\left(\frac{x}{W}\right)}{\sqrt{1-\left(\frac{x}{W}\right)^2}}$$

$$f_{yk}(x) = U_k\left(\frac{x}{W}\right) \qquad (20)$$

where $T_k(y)$ and $U_k(y)$ are the Chebyshev's polynomials of the first and second kind, respectively.

Preliminary computations show that $N_x = N_y = 2$ in (19) is sufficient for deriving accurate results for finite metallization thickness just as in the case of zero metallization thickness [3].

Figure 4 shows the effect of the metallization thickness t on the effective dielectric constant and the characteristic impedance in a unilateral fin line. The effective dielectric constant and the characteristic impedance z_0 are defined as

$$\left(\beta_0/\omega\sqrt{\varepsilon_0\mu_0}\right)^2$$

$$z_0 = \frac{V_0^2}{2P_{ave}} \tag{21}$$

where V_0 is the voltage between the fins and P_{ave} is the average power flow along the y-direction.

The finite thickness reduces the propagation constant in the higher-frequency range as it does in the open slot line [5], because in these frequency ranges the fields are concentrated near the gap in the fin-line and it acts similar to an open slot line. In contrast, a fin-line behaves as a ridged waveguide near the cutoff frequency, and consequently, the thicker its diaphragm, the lower its cutoff frequency [7].

Figure 5 shows the effect of the metallization thickness of a bilateral fin-line. The results for the limiting case of $t = 0$, i.e., zero metallization thickness, are compared with those published by Schmidt and Itoh [1], and the agreement is quite good.

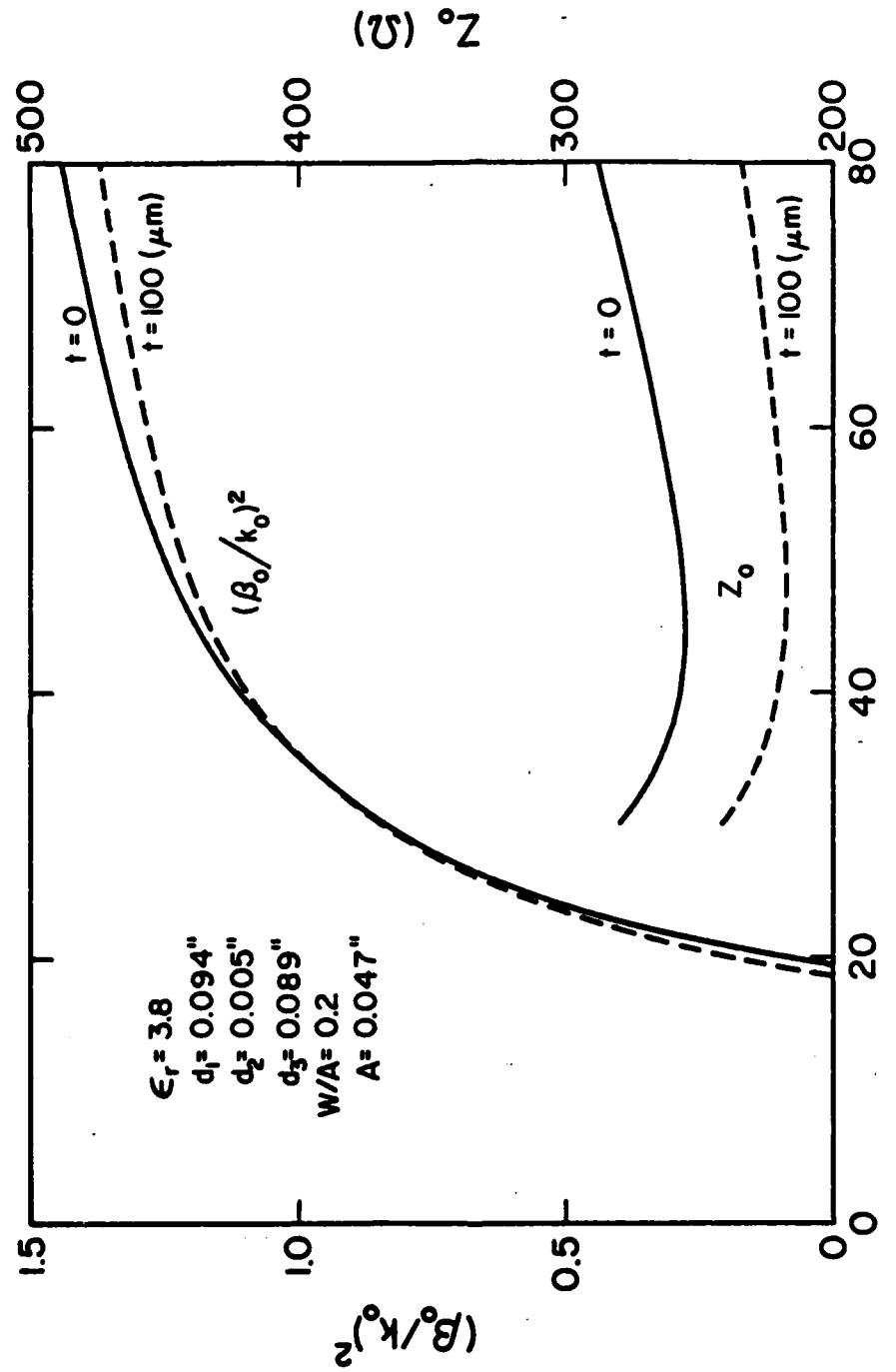

Figure 4. Propagation characteristics of unilateral fin line.

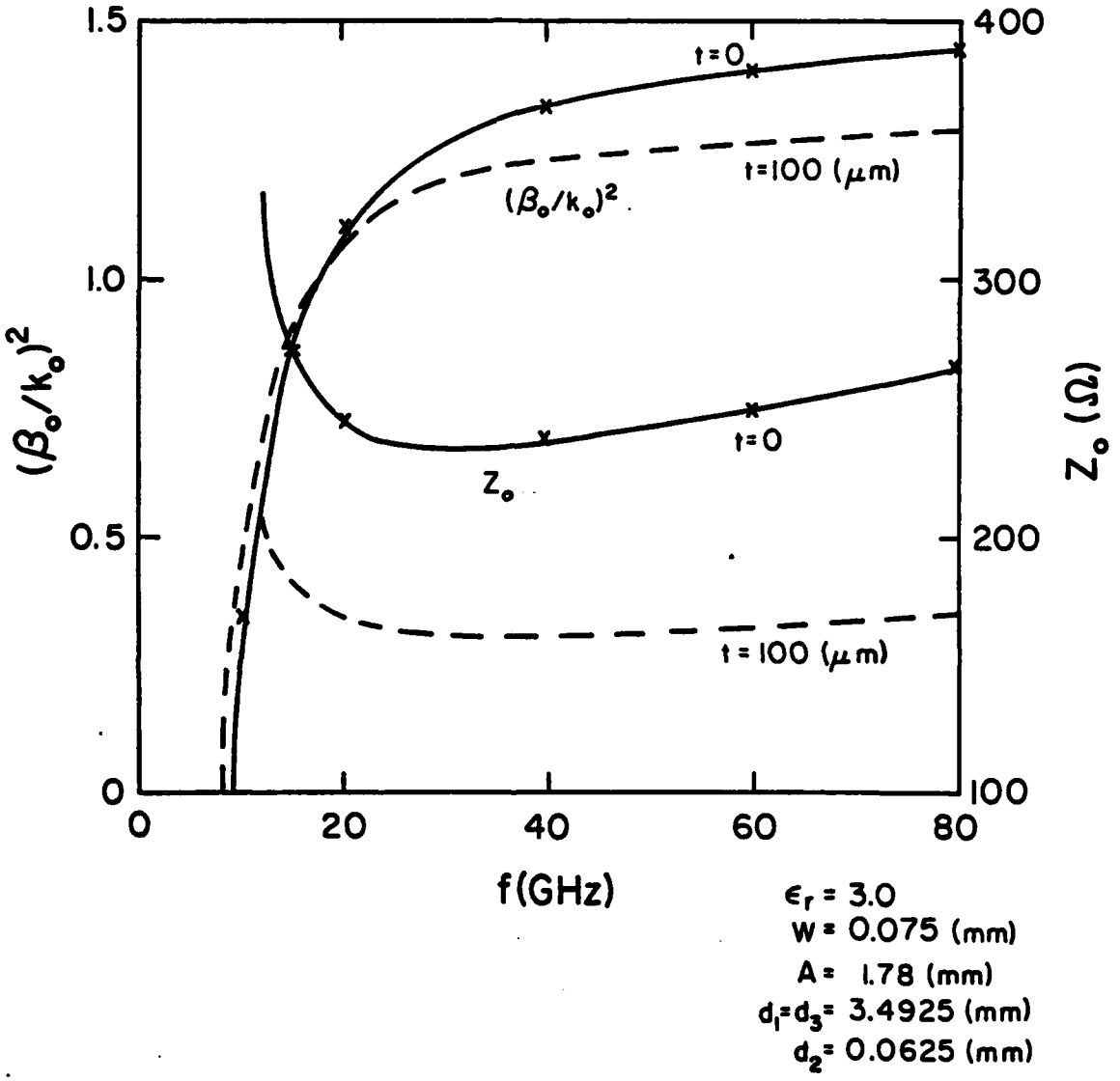

Figure 5. Propagation characteristics of bilateral fin line.

IV. CONCLUSIONS

In this paper, the hybrid mode formulation was used to analyze fin-line structures with finite metallization thicknesses. This formulation used in conjunction with the equivalent circuit analysis is considerably simpler than the conventional Green's function approach. This method itself is quite general and can be applied to different types of fin-line structures by a simple modification of equivalen circuits which can be obtained easily.

Numerical results are presented to show the effects of finite metallization thickness on the propagation characteristics of unilateral and bilateral fin-line structures.

REFERENCES

[1] L. P. Schmidt and T. Itoh, "Spectral domain analysis of dominant and higher order modes in fin-lines," IEEE Trans. Microwave Theory Tech., vol. MTT-28, pp. 981-985, September 1980.

[2] L. P. Schmidt, T. Itoh, and H. Hofman, "Characteristics of unilateral fin-line structures with arbitrary located slots," IEEE Trans. Microwave Theory Tech., vol. MTT-29, pp. 352-355, April 1981.

[3] Y. Hayashi, E. Farr, S. Wilson and R. Mittra, "Analysis of dominant and higher-order modes in unilateral fin lines," AEU, vol. 37, no. 3/4, pp. 117-122, March-April 1983.

[4] A. Beyer, "Analysis of characteristics of an earthed fin line," IEEE Trans. Microwave Theory Tech., vol. MTT-29, pp. 676-680, July 1981.

[5] T. Kitazawa, Y. Hayashi, and M. Suzuki, "Analysis of the dispersion characteristic of slot line with thick metal coating," IEEE Trans. Microwave Theory Tech., vol. MTT-28, pp. 387-392, April 1980.

[6] T. Kitazawa, Y. Hayashi and M. Suzuki, "A coplanar waveguide with thick metal coating," IEEE Trans. Microwave Theory Tech., vol. MTT-24, pp. 604-608, September 1976.

[7] J. R. Pyle, "The cutoff wavelength of the TE_{10} mode in ridged rectangular waveguide of any aspect ratio," IEEE Trans. Microwave Theory Tech., vol. MTT-14, pp. 175-183, April 1966.

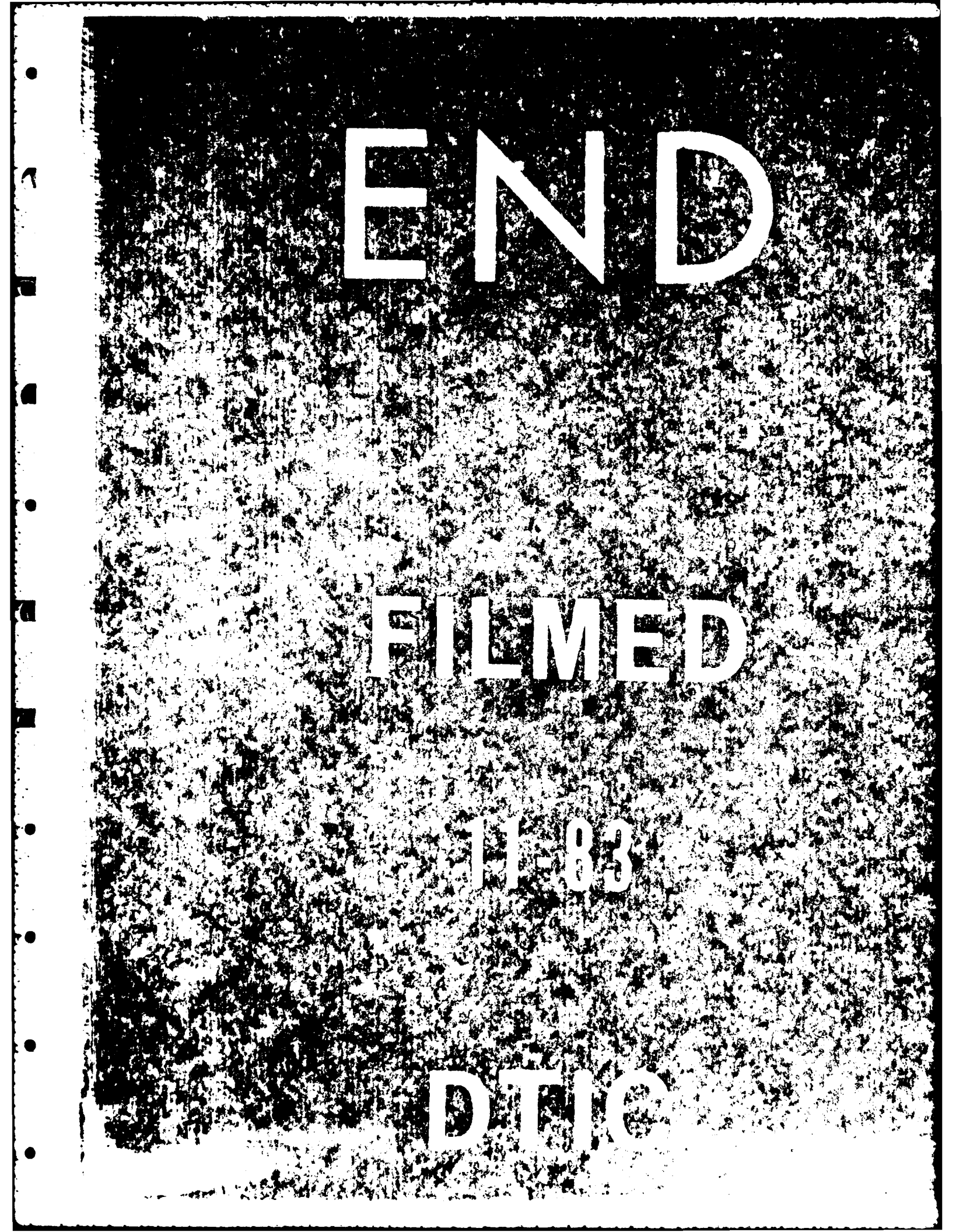
END
FILMED
11-83
DTIC